

Defective Glycogenesis Contributes Toward the Inability to Suppress Hepatic Glucose Production in Response to Hyperglycemia and Hyperinsulinemia in Zucker Diabetic Fatty Rats

Tracy P. Torres,¹ Yuka Fujimoto,¹ E.P. Donahue,¹ Richard L. Printz,¹ Karen L. Houseknecht,² Judith L. Treadway,² and Masakazu Shiota¹

OBJECTIVE—Examine whether normalizing net hepatic glycogenesis restores endogenous glucose production and hepatic glucose phosphorylation in response to diabetic levels of plasma glucose and insulin in Zucker diabetic fatty rats (ZDF).

RESEARCH DESIGN AND METHODS—Hepatic glucose and intermediate fluxes ($\mu\text{mol} \cdot \text{kg}^{-1} \cdot \text{min}^{-1}$) were measured with and without a glycogen phosphorylase inhibitor (GPI) using [$2\text{-}^3\text{H}$]glucose, [$3\text{-}^3\text{H}$]glucose, and [$\text{U-}^{14}\text{C}$]alanine in 20 h-fasted conscious ZDF and their lean littermates (ZCL) under clamp conditions designed to maintain diabetic levels of plasma glucose and insulin.

RESULTS—With infusion of GPI into ZDF (ZDF-GPI+G), compared with vehicle infused ZDF (ZDF-V), high glycogen phosphorylase activity was decreased and low synthase I activity was increased to that of ZCL. Low net glycogenesis from plasma glucose rose to 75% of ZCL levels (4 ± 1 in ZDF-V, 18 ± 1 in ZDF-GPI+G, and 24 ± 2 in ZCL) and phosphoenolpyruvate 260% (4 ± 2 in ZDF-V, 16 ± 1 in ZDF+GPI-G, and 6 ± 2 in ZCL). High endogenous glucose production was suppressed with GPI infusion but not to that of ZCL (46 ± 4 in ZDF-V, 18 ± 4 in ZDF-GPI+G, and -8 ± 3 in ZCL). This was accompanied by reduction of the higher glucose-6-phosphatase flux (75 ± 4 in ZDF-V, 41 ± 4 in ZDF-GPI+G, and 86 ± 12 in ZCL) and no change in low glucose phosphorylation or total gluconeogenesis.

CONCLUSIONS—In the presence of hyperglycemic-hyperinsulinemia in ZDF, reduced glycolytic flux partially contributes to a lack of suppression of hepatic glucose production by failing to redirect glucose-6-phosphate flux from production of glucose to glycogen but is not responsible for a lower rate of glucose phosphorylation. *Diabetes* 60:2225–2233, 2011

D iabetic hyperglycemia is in part associated with a lesser suppression of net hepatic glucose production and a defect in hepatic glucose uptake in response to increased plasma glucose and insulin (1–4). These defects are accompanied by reduced hepatic glycogen synthesis (5–7).

The flux from glucose to glycogen has two highly regulated steps, glucose phosphorylation by glucokinase (GK) and the formation of a glycosidic bond between C1 of the activated glucose uridine 5'-diphosphate (UDPG) and C4 of a terminal glucose residue of glycogen by glycogen synthase (GS) (8). Basu et al. (5,6) showed that lower net splanchnic glucose uptake measured during a hyperglycemic-hyperinsulinemic clamp in type 2 diabetic subjects when compared with nondiabetic subjects is associated with a proportionate decrease in both the flux through the UDPG pool and the percentage of extracellular glucose contributing to glycogen synthesis via the direct pathway. Mevorach et al. (9) reported glucose cycling fails to increase even when the concentration of circulating glucose doubles. We (10–13) reported that in Zucker diabetic fatty rats (ZDF), a widely used genetic model of obese type 2 diabetes, the failure to suppress endogenous glucose production (EGP) and to increase in flux from glucose to glycogen in response to a rise in plasma glucose and insulin is associated with defects in allosteric activation of GK during an early stage of diabetes and decreased expression of GK during a late stage of diabetes. These observations suggest that insufficient suppression of net hepatic glucose production and a defect in hepatic glucose uptake in response to increased plasma glucose and insulin seen in type 2 diabetes results, at least partly, from a failure to enhance glucose phosphorylation mediated by GK. On the other hand, Cline et al. (14) reported that activation of GS by treatment with an inhibitor of glycogen synthase kinase-3 improves glucose disposal during an oral glucose tolerance test in ZDF, which indicated a defect in net glycogenesis, regardless of any defect in glucose phosphorylation in this diabetic model (10–12).

To assess the contribution of a defect in net glycogenesis and glucose phosphorylation to the blunted response of hepatic glucose flux to hyperglycemia and hyperinsulinemia in ZDF, we examined the effects of restoring net glycogenesis by treatment with a glycogen phosphorylase inhibitor (GPI).

From the ¹Department of Molecular Physiology and Biophysics, Vanderbilt University School of Medicine, Nashville, Tennessee; and ²Pfizer Inc., Groton, Connecticut.

Corresponding author: Masakazu Shiota, masakazu.shiota@vanderbilt.edu.

Received 6 August 2009 and accepted 11 June 2011.

DOI: 10.2337/db09-1156

This article contains Supplementary Data online at <http://diabetes.diabetesjournals.org/lookup/suppl/doi:10.2337/db09-1156/-/DC1>.

© 2011 by the American Diabetes Association. Readers may use this article as long as the work is properly cited, the use is educational and not for profit, and the work is not altered. See <http://creativecommons.org/licenses/by-nc-nd/3.0/> for details.

RESEARCH DESIGN AND METHODS

Surgical procedure. Six-week-old male ZDF (ZDF/GmiCrl-*fa/fa*) and their lean littermates (ZCL) were purchased from Charles River Laboratories, Inc. (Wilmington, MA). Rats were fed with Formulab Diet 5008 (Purina LabDiet; Purina Mills, Inc., Richmond, IN) and were given water ad libitum in an environmentally controlled room with a 12-h light/dark cycle. At 12 weeks of age, 2 weeks prior to the experiment, surgery was performed to place a sterile silicone rubber catheter (0.51 mm internal diameter and 0.94 mm outer diameter) in an ileal vein, the left common carotid artery, and the right external jugular vein as described previously (10–13).

Studies for measuring glucose kinetics. At 14 weeks of age, the animals were fasted for 20 h prior to each study. Each study consisted of a 90-min tracer equilibration period (–150 to –60 min), a 1-h control period (–60 to 0 min), and a 3-h test period (0 to 180 min). At –150 min, both [$2\text{-}^3\text{H}$]glucose and [$3\text{-}^3\text{H}$]glucose were given as a bolus (60 μCi) and then infused at 0.6 $\mu\text{Ci}/\text{min}$ through the jugular vein catheter during the experimental period. During the test period, change in the specific activities (SAs) of [$2\text{-}^3\text{H}$] and [$3\text{-}^3\text{H}$]glucose in plasma were minimized by varying the tracer infusion rate based on an algorithm obtained from preliminary studies, thereby reducing non-steady-state errors associated with the estimation of glucose R_a that may arise from intercompartmental tracer concentration gradients between plasma and interstitial compartments (15). At 170 min, [$U\text{-}^{14}\text{C}$]alanine was given as a bolus (100 μCi) and then infused continuously at 10 $\mu\text{Ci}/\text{min}$ for 10 min through the arterial catheter. During the test period, in the first group of ZDF (ZDF-V), the vehicle (25% sulphobutylether β -cyclodextrin solution) was infused into systemic circulation through the jugular vein catheter at 20 $\mu\text{L} \cdot \text{kg}^{-1} \cdot \text{min}^{-1}$. In the second group of ZDF (ZDF-GPI), GPI (CP-368296; Pfizer Inc., Groton, CT) was continuously infused at 104 $\mu\text{g} \cdot \text{kg}^{-1} \cdot \text{min}^{-1}$ after a bolus infusion of 15 $\text{mg} \cdot \text{kg}^{-1} \cdot \text{min}^{-1}$ at 0 min. In the third group of ZDF (ZDF-GPI+G), in addition to the infusion of GPI as described for the second group, 50% glucose solution was infused through the jugular vein catheter at a variable rate to maintain a basal concentration. In the fourth group (ZCL), hyperglycemic-hyperinsulinemic clamps were performed to maintain plasma glucose, insulin, and glucagon levels at levels seen in the ZDF. At 0 min when glucose infusion was initiated, somatostatin was infused at 5 $\mu\text{g} \cdot \text{kg}^{-1} \cdot \text{min}^{-1}$ through the jugular vein catheter while insulin and glucagon were also infused at 5 $\text{mU} \cdot \text{kg}^{-1} \cdot \text{min}^{-1}$ and 3 $\text{ng} \cdot \text{kg}^{-1} \cdot \text{min}^{-1}$, respectively, into the portal vein through the ileal vein catheter. Blood samples were taken through the arterial catheter. At each sampling time, to maintain the hematocrit levels, erythrocytes were washed and resuspended with saline and given back to each animal. At the end of each experiment, the left liver lobe and skeletal muscle (vastus lateralis) were frozen in situ as described previously (10–13).

Determination of body mass of glucose and space of glucose distribution. Body mass of glucose (Gmass) was measured using [$2\text{-}^3\text{H}$]glucose as tracer according to Katz et al. (16). [$2\text{-}^3\text{H}$]glucose (34 μCi) was administered by a single injection through the jugular vein catheter. Blood samples (150 μL) were withdrawn through the carotid artery catheter at increasing time intervals after the tracer injection, from a few minutes initially to ~30 min after 90 min of a 3-h experimental period.

All experiments were conducted in accordance with the *Guide for the Care and Use of Laboratory Animals* of both the U.S. Department of Agriculture and the National Institutes of Health, and all protocols were approved by the Vanderbilt University Institutional Animal Care and Use Committee.

Metabolites in blood and tissue. Glycogen content in liver and skeletal muscle, glucose-6-phosphate (G-6-P) concentration in the liver, and plasma glucose, insulin, glucagon, and plasma SAs of [$2\text{-}^3\text{H}$], [$3\text{-}^3\text{H}$], and [^{14}C]glucose ([$2\text{-}^3\text{H}$]SA, [$3\text{-}^3\text{H}$]SA, and [^{14}C]SA, respectively) were determined as previously described (10–13,17). To determine [$2\text{-}^3\text{H}$]SA, [$3\text{-}^3\text{H}$]SA, and [^{14}C]SA, plasma was deproteinized using $\text{Ba}(\text{OH})_2$ and ZnSO_4 . After centrifugation, the supernatant was passed through a cation resin (Dowex 50WX8 100–200 mesh; Sigma-Aldrich, Inc., St. Louis, MO) and an anion resin (Amberlite IRA-67; Sigma-Aldrich, Inc.) to remove ^3H - and/or ^{14}C -labeled lactate, pyruvate, and amino acids. Glycogen was extracted from liver and skeletal muscle and degraded to glucose using amyloglucosidase. [$2\text{-}^3\text{H}$] and [$3\text{-}^3\text{H}$]glucose radioactivity in plasma glucose, as well as glycogen-glucose, were determined by selective enzymatic detritiation of [$2\text{-}^3\text{H}$]glucose (10–13). Subtraction of [$3\text{-}^3\text{H}$]glucose radioactivity from total ^3H radioactivity yielded [$2\text{-}^3\text{H}$]glucose radioactivity. Overall completion of detritiation of [$2\text{-}^3\text{H}$]glucose using this method was 97.3 \pm 0.4 ($n = 5$), whereas 99.7 \pm 0.4 ($n = 5$) of [$3\text{-}^3\text{H}$]glucose remained intact. The liver content of UDPG and phosphoenolpyruvate (PEP) were obtained through two sequential chromatographic separations, and the radioactivity of ^3H and ^{14}C in each fraction was measured (11,12).

Calculations. Body glucose distribution volume (V_D) was calculated according to the method reported by Katz et al. (16). The zero-time intercept value of [$2\text{-}^3\text{H}$]SA in plasma glucose was obtained from a semilogarithmic plot

of time after a single injection of [$2\text{-}^3\text{H}$]glucose versus [$2\text{-}^3\text{H}$]SA in plasma glucose. Gmass was calculated as: $\text{Gmass} (\mu\text{mol}/\text{kg}) = \text{amount of injected } [2\text{-}^3\text{H}]\text{glucose} (\text{dpm}/\text{kg}) / \text{the zero-time intercept value of } [2\text{-}^3\text{H}]\text{SA in plasma glucose} (\text{dpm}/\mu\text{mol})$. V_D was calculated as: $V_D = \text{Gmass} (\mu\text{mol}/\text{kg body wt}) / \text{plasma glucose} (\mu\text{mol}/\text{mL})$. V_D was determined to be 292 mL/kg body wt in ZCL and 275 mL/kg body wt in ZDF (Table 1). The calculations of metabolite fluxes and the assumptions related to the calculations are presented in the Supplementary Appendix.

Statistical analyses. Data are expressed as means \pm SE. For the time-course data, significant differences between groups were analyzed using two-way repeated-measures ANOVA. Otherwise, significant differences between groups were analyzed using one-way ANOVA or Student t test. Differences were considered significant at $P < 0.05$.

RESULTS

Basal metabolic profiles. In ZDF, compared with ZCL, basal plasma glucose and insulin levels were three to four times higher, whereas plasma glucagon levels were similar (Fig. 1 and Table 2). EGP and glucose cycling rates and glucose-6-phosphatase (G-6-Pase) flux rates tended to be higher (Fig. 2 and Table 2). Among the three groups of ZDF, we measured no significant differences in plasma levels of glucose, insulin, and glucagon or in the [$3\text{-}^3\text{H}$]R_d and the rates of EGP, glucose cycling, and G-6-Pase flux (Figs. 1 and 2 and Table 2).

Metabolic profiles in the presence of both hyperglycemia and hyperinsulinemia. During the test period, in ZCL, plasma glucose and insulin levels were raised to that of basal levels in ZDF (Fig. 1). The infusion rates of tracers were increased stepwise (Fig. 2A and B) to minimize SA changes in [$2\text{-}^3\text{H}$] and [$3\text{-}^3\text{H}$]glucose (Fig. 2C and D). [$3\text{-}^3\text{H}$]R_d increased from four- to fivefold (Fig. 2E), and EGP was completely suppressed (Fig. 2F) with increased G-6-Pase flux (G-6-P to glucose) (Fig. 2H). Glucose cycling increased fivefold (Fig. 2G). Fractional contributions of plasma glucose and PEP to UDPG flux were 78 \pm 3 and 20 \pm 2%, respectively (Fig. 3D). Newly synthesized glycogen from plasma glucose via the direct pathway and PEP were 108 \pm 11 μmol and 29 \pm 7 μmol per gram of liver, respectively (Fig. 3F). Newly synthesized glycogen (Fig. 3F; 142 \pm 12 μmol glucose/g) occupied 90% of stored glycogen (Fig. 3E; 155 \pm 20 μmol glucose/g liver).

In ZDF, the infusion of vehicle (ZDF-V) did not alter [$3\text{-}^3\text{H}$]R_d, glucose cycling, EGP, and G-6-Pase flux from that of basal levels (Fig. 2). Compared with ZCL, glucose cycling rate was significantly lower (Fig. 2G), whereas G-6-Pase flux rate (Fig. 2F) was similar during the last 60 min of the test period. In addition, and as shown in Fig. 3, G-6-P (110 \pm 22 vs. 94 \pm 16 nmol/g liver) and UDPG contents were similar (208 \pm 15 vs. 207 \pm 21 nmol/g liver) but PEP content was markedly lower (7 \pm 1 vs. 29 \pm 5 nmol/g liver). The percent contribution of plasma glucose (50 \pm 2%) to UDPG flux was significantly lower, whereas the fractional contribution of PEP (47 \pm 4%) was more than doubled (Fig. 3D and Table 3). The amount of newly synthesized glycogen (32 \pm 5 μmol glucose/g liver), the amount of plasma glucose incorporated via the direct pathway (16 \pm 7 μmol glucose/g liver), and the amount of PEP

TABLE 1
Body Gmass and space of glucose distribution in ZDF and ZCL

Animals	Body weight (g)	PG (mmol/L)	[$2\text{-}^3\text{H}$]I $\times 10^7$ dpm/kg	[$2\text{-}^3\text{H}$]SA $\times 10^7$ dpm/mol	Gmass (mmol/kg)	V_D (mL/kg)
ZCL	365 \pm 9	6.7 \pm 0.5	15.9 \pm 1.3	8.12 \pm 0.65	1.96 \pm 0.16	292 \pm 9
ZDF	395 \pm 12	26.5 \pm 2.1	15.4 \pm 1.7	2.11 \pm 0.26	7.29 \pm 0.80	275 \pm 11

PG, plasma glucose; [$2\text{-}^3\text{H}$]I, given amount of [$2\text{-}^3\text{H}$]glucose; [$2\text{-}^3\text{H}$]SA, zero-time intercept value of [$2\text{-}^3\text{H}$] specific activity in plasma glucose. Values are means \pm SE for five animals in each group.

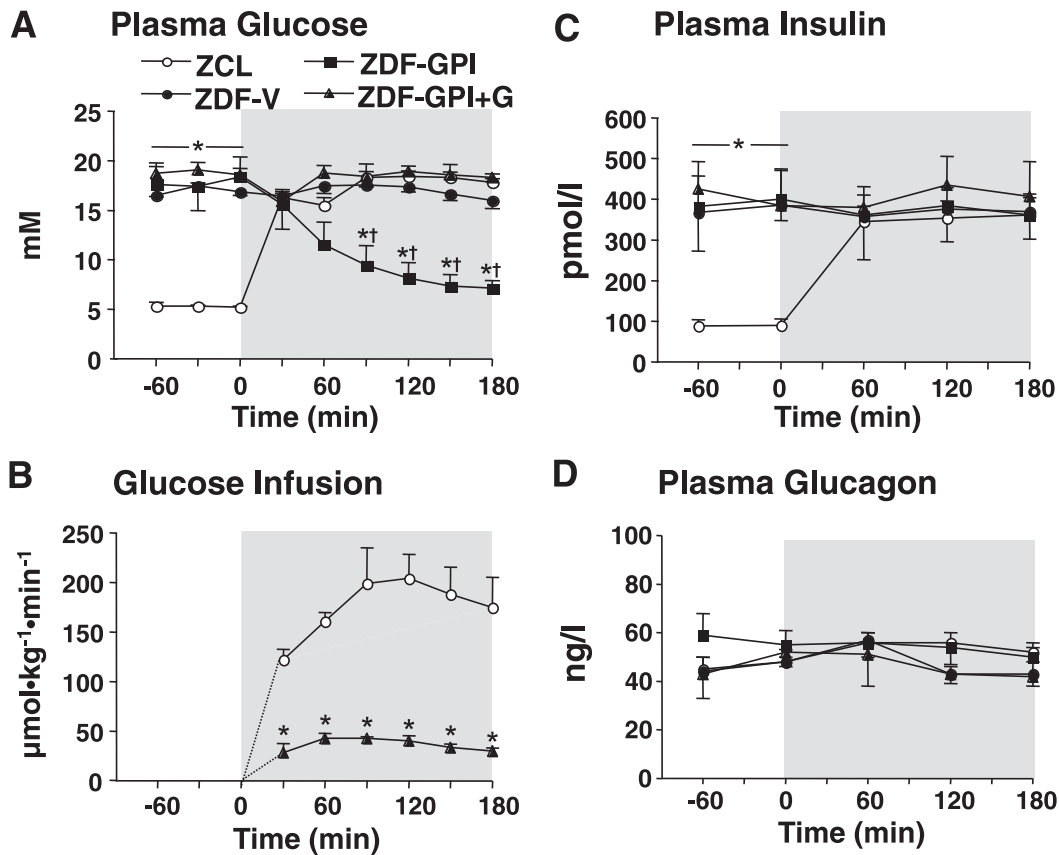


FIG. 1. Plasma levels of glucose, insulin, glucagon, and glucose infusion rates prior to and during infusion of vehicle or GPI in 20-h fasted conscious ZDF and ZCL. Data are means \pm SE for five experiments. *Significantly different from ZCL at identical time points ($P < 0.05$). †Significantly different from ZDF-V at identical time points ($P < 0.05$).

($15 \pm 4 \mu\text{mol glucose/g liver}$) incorporated were markedly lower (Fig. 3F). Although the content of glycogen ($269 \pm 27 \mu\text{mol glucose/g liver}$) nearly doubled (Fig. 3E), the newly synthesized glycogen was only 20% of the total glycogen.

In response to GPI infusion (ZDF-GPI), plasma glucose levels decreased from 18 ± 2 to $7 \pm 1 \text{ mmol/L}$ by 180 min without altering plasma insulin and glucagon levels (Fig. 1). The $[2\text{-}^3\text{H}]\text{SA}$ and $[3\text{-}^3\text{H}]\text{SA}$ were kept constant (Fig. 2C and D) by decreasing the infusion rate of these tracers (Fig. 2A and B). Compared with ZDF-V, $[3\text{-}^3\text{H}]\text{R}_d$, EGP, glucose cycling, and G-6-Pase flux were decreased $\sim 50\%$ by the end of the test period (Fig. 2). Hepatic contents of G-6-P and UDPG (31 ± 13 and $126 \pm 24 \text{ nmol/g liver}$, respectively) were reduced by 70 and 40%, respectively (Fig. 3A and C). The percent contribution to UDPG derived from plasma glucose ($39 \pm 4\%$) was significantly lower than that found in

ZDF-V, whereas that derived from PEP ($58 \pm 6\%$) tended to be higher (Fig. 3D). However, the amount of plasma glucose incorporated via the direct pathway ($47 \pm 7 \mu\text{mol glucose/g liver}$) and derived from PEP ($69 \pm 7 \mu\text{mol glucose/g liver}$) incorporated into glycogen were increased three- and five-fold, respectively (Fig. 3F). Glycogen content ($386 \pm 8 \mu\text{mol glucose/g liver}$) was significantly increased (Fig. 3E) and newly synthesized glycogen ($119 \pm 12 \mu\text{mol glucose/g liver}$) was 30% of total glycogen. When compared with ZCL, ZDF-GPI had similar levels of newly synthesized glycogen, but approximately half the amount of plasma glucose was incorporated via the direct pathway into glycogen, whereas that derived from PEP doubled (Fig. 3F).

Infusion of glucose along with GPI in ZDF (ZDF-GPI+G) was done to maintain glycemia at basal ZDF levels. Under these conditions, the $[3\text{-}^3\text{H}]\text{R}_d$ and rates of EGP, glucose

TABLE 2

Plasma hormones, plasma glucose, and hepatic glucose flux in 14-week-old ZCL and ZDF as measured basal

	ZCL	ZDF-V	ZDF-GPI	ZDF-GPI+G
Plasma insulin (pmol/L)	89 ± 15	$386 \pm 84^*$	$400 \pm 74^*$	$384 \pm 37^*$
Plasma glucagon (ng/L)	48 ± 2	48 ± 2	55 ± 6	52 ± 1
Plasma glucose (mmol/L)	5.2 ± 0.3	$16.8 \pm 0.3^*$	$18.4 \pm 2.0^*$	$18.6 \pm 0.7^*$
Endogenous glucose production	41 ± 5	48 ± 2	44 ± 4	48 ± 3
Glucose cycling rates	21 ± 3	32 ± 5	$45 \pm 4^*$	35 ± 4
G-6-Pase flux	62 ± 6	$80 \pm 4^*$	$89 \pm 7^*$	$83 \pm 3^*$

Glucose cycling rate and G-6-Pase flux are the minimal estimates that were calculated with assumption that exchange of ^3H at the second position of G-6-P with hydrogen of bulk water is 100%. The values for flux rates are described in $\mu\text{mol} \cdot \text{kg}^{-1} \cdot \text{min}^{-1}$. The values are averages \pm SE of five experiments. *Significant difference from the corresponding values of the ZCL group ($P < 0.05$).

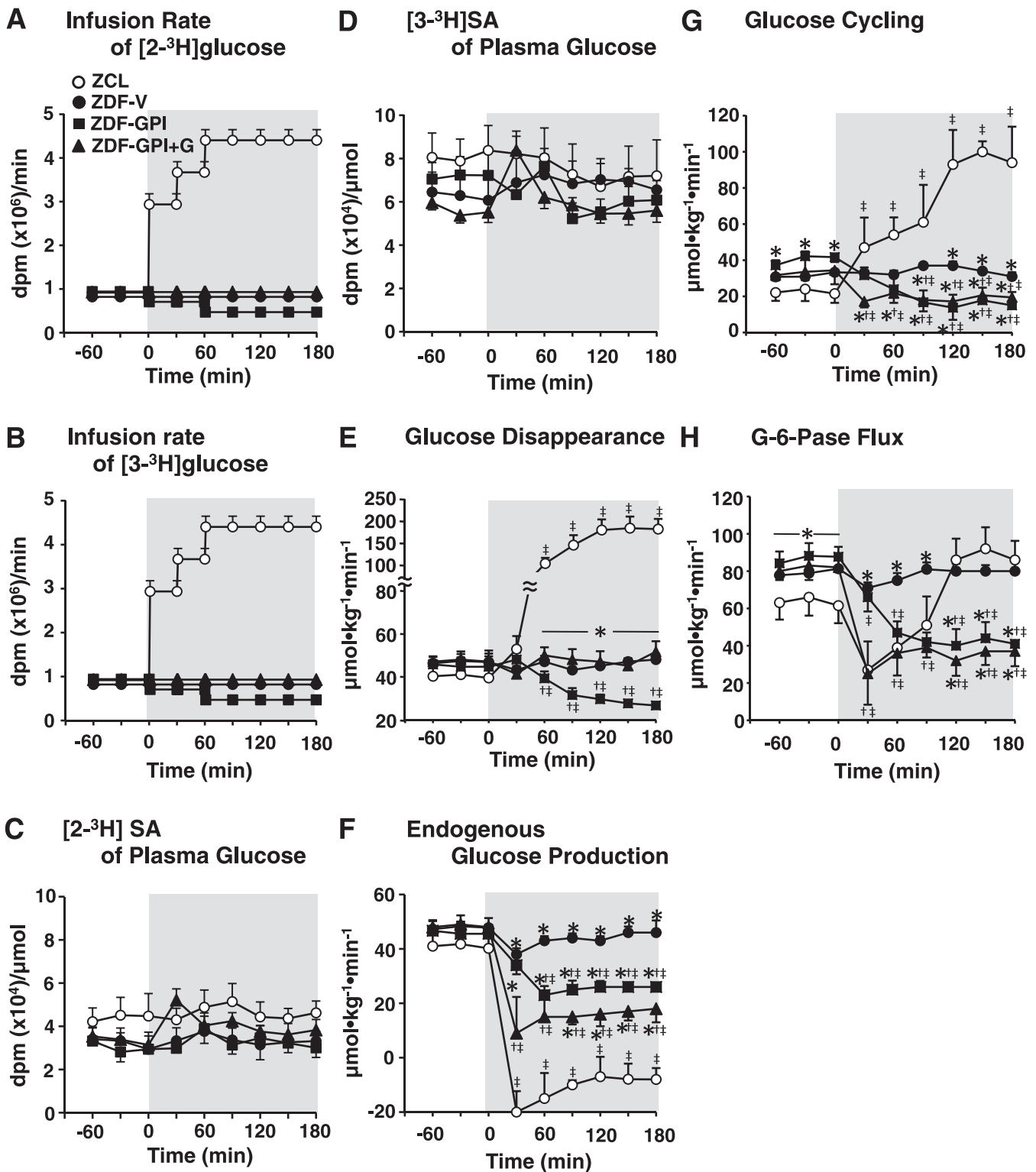


FIG. 2. Glucose R_a , EGP rates, minimally estimated glucose cycling rates, and minimally estimated G-6-Pase flux rates prior to and during infusion of vehicle or GPI in 20-h fasted conscious ZDF and ZCL. Data are means \pm SE for five experiments. *Significantly different from ZCL at identical time points ($P < 0.05$). †Significantly different from ZDF-V group at the identical time points ($P < 0.05$). ‡Significantly different from the control period within the same group ($P < 0.05$).

cycling, and G-6-Pase flux were rapidly decreased within 30 min and thereafter returned partially (Fig. 2). The rapid decrease in these parameters was the result of a rapid rise in the [2-³H]SA and [3-³H]SA that was not accompanied by increased infusion rates of these tracers (Fig. 2C and D);

therefore, the rise of the [2-³H]SA and [3-³H]SA might be because of a technical problem. At the termination of the study, no significant differences from only GPI infusion (ZDF-GPI) were observed with any of the measured parameters (Figs. 2 and 3 and Table 2).

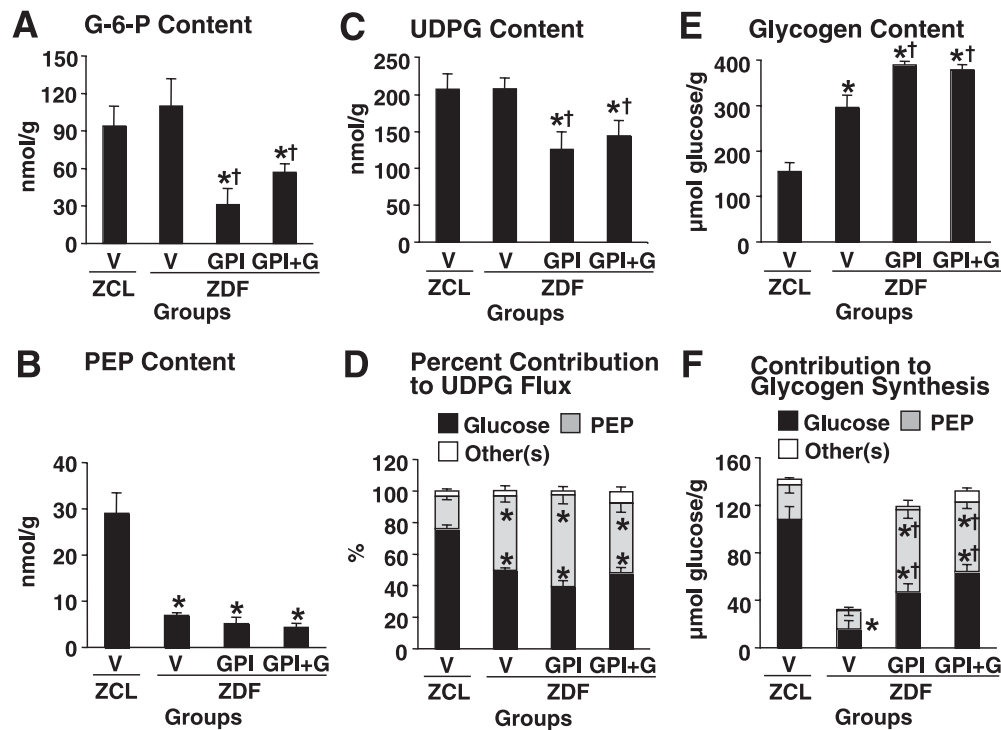


FIG. 3. Hepatic contents of G-6-P, UDPG, PEP, and glycogen; fractional contribution of plasma glucose, PEP, and the other metabolites to UDPG flux and glycogen synthesis at the end of the test period. Data are means \pm SE for five experiments. *Significantly different from ZCL group ($P < 0.05$). †Significantly different from ZDF-V group ($P < 0.05$).

Effect of GPI on activities of glycogen phosphorylase, GS, GK, and G-6-Pase. In ZDF-V compared with ZCL, glycogen phosphorylase a (GP_a) activity was significantly higher (units/g liver; 14.2 ± 2.6 in ZDF-V vs. 6.8 ± 1.6 in ZCL) and, in contrast, glycogen synthase I (GSI) activity was significantly lower (units/g liver; 0.14 ± 0.01 in ZDF-V vs. 0.24 ± 0.04 in ZCL) (Fig. 4). With GPI treatment of ZDF (ZDF-GPI), GP_a activity decreased (7.7 ± 2.2 units/g liver) and GSI increased (0.34 ± 0.04 units/g liver). In addition, the GS activity ratio (active form/total activity) increased to the levels seen in ZCL. The maintenance of hyperglycemia along with GPI infusion (ZDF-GPI+G) tended to enlarge GPI-induced changes in GP activity (6.4 ± 1.6 units/g liver), GSI activity (0.45 ± 0.17 units/g liver), or the GS activity ratio (0.32 ± 0.07). GK and G-6-Pase activity in the liver were not significantly different among ZCL and ZDF. **Estimated G-6-P flux in the liver during test period.** The difference in G-6-P flux within the liver between ZCL and ZDF, as well as changes in flux in ZDF when net glycogenesis is increased, is listed in Table 3 and shown schematically in Fig. 5.

When plasma glucose and insulin levels were raised to that in ZDF, in ZCL, EGP was completely suppressed. Total flux toward G-6-P pool consisted of several major fractions from plasma glucose (78%), PEP (20%), and the other source (glycogen and glycerol; 2%). In addition, 26% of G-6-P derived from plasma glucose and 35% derived from PEP were stored as glycogen, whereas the rest recycled back to glucose or was released as glucose, respectively. GK flux (glucose to G-6-P) was higher than G-6-Pase flux.

In ZDF-V in which EGP was sustained, compared with ZCL, total flux toward the G-6-P pool, consisting of fractions from plasma glucose (50%), PEP (47%), and others (3%), was significantly lower. Total efflux from G-6-P pool flowed

primarily toward glucose (90%) and glycogen (10%). Of the G-6-P derived from plasma glucose, only 10% was stored as glycogen and the rest (90%) was recycled to glucose. Of the G-6-P derived from PEP, 10% was stored as glycogen and the rest (90%) was released as glucose. GK flux was $\sim 30\%$ of that in ZCL, whereas G-6-Pase flux was similar. GK flux was lower than G-6-Pase flux contrary to ZCL. The flux from PEP to G-6-P was 70% higher.

With GPI treatment (ZDF-GPI), without significant changes in total flux toward G-6-P pool, EGP was decreased by 44%. This decrease was associated with a change in flow of G-6-P with a 40% decrease in the flux of G-6-P toward glucose and a 4.5-fold increase in the flux of G-6-P toward glycogen. The G-6-P fractions derived from plasma glucose tended to decrease and in contrast, PEP tended to increase. As seen in ZDF-GPI+G, maintaining hyperglycemia with GPI treatment tended to lower EGP, increase G-6-P derived from plasma glucose, and decrease that from PEP slightly. It increased glycogen synthesis from plasma glucose and in contrast, decreased that from PEP slightly, whereas it did not alter total glycogen synthesis.

Estimating whole body glucose kinetics along with intracellular intermediate fluxes using tracers involves certain assumptions. Estimates of G-6-Pase flux and GK flux (glucose phosphorylation) are dependent upon the measurement of glucose cycling rate using [$2\text{-}^3\text{H}$]glucose, which involves an assumption that exchange by hexose 6-phosphate isomerase of G-6-P hydrogen 2 with that of bulk water is 100% complete before proceeding down any pathways (18,19). Our data from liver predict $\sim 50\%$ exchange completion. Such a low exchange is likely not an error in analytical processing of the sample because the exchange measured in skeletal muscle was $\sim 90\%$ ($89 \pm 8\%$ in ZCL, $88 \pm 7\%$ in ZDF, $91 \pm 2\%$ in ZDF-GPI, and $89 \pm 5\%$

TABLE 3

Hepatic glucose flux, plasma hormones, enzyme activities, and metabolites in 14-week-old ZCL and ZDF as measured during test period

	ZCL	ZDF-V	ZDF-GPI	ZDF-GPI+G
Plasma insulin (pmol/L)	361 ± 43	369 ± 43	361 ± 60	406 ± 86
Plasma glucagon (ng/L)	52 ± 4	43 ± 4	50 ± 4	42 ± 4
Plasma glucose (mmol/L)	17.8 ± 0.8	16.0 ± 0.8	7.1 ± 0.8*†	18.3 ± 0.3
[2- ³ H]R _a	288 ± 46	75 ± 4*	47 ± 2*†	67 ± 8*‡
[3- ³ H]R _a	194 ± 26	46 ± 4*	26 ± 3*†	48 ± 5*‡
GIR	175 ± 28	0	0	30 ± 3*
EGP	-8 ± 3	46 ± 4*	26 ± 3*†	18 ± 4*†
Detritiation of [2- ³ H]G-6-P (%)	41 ± 4	52 ± 5	56 ± 5	55 ± 3
Contribution to form UDPG (%)				
Plasma glucose	78 ± 3	50 ± 2*	39 ± 4*†	48 ± 3*
PEP	20 ± 3	47 ± 4*	58 ± 6*	44 ± 6*
Others	2 ± 2	3 ± 3	3 ± 3	8 ± 6
Glycogen synthesis				
Total	31 ± 4	8 ± 6*	35 ± 4	37 ± 5
From plasma glucose	24 ± 2	4 ± 1*	13 ± 1*†	18 ± 1*†‡
From PEP	6 ± 2	4 ± 2	21 ± 3*†	16 ± 1*†
From others	1 ± 0	0 ± 5	1 ± 1	3 ± 3
Minimal estimation				
Glucose cycling rates	94 ± 21	29 ± 3*	21 ± 2*†	23 ± 6*†
GK flux	118 ± 16	33 ± 3*	34 ± 3*	41 ± 3*
G-6-Pase flux				
Total	86 ± 12	75 ± 4	47 ± 2*†	41 ± 4*†
From plasma glucose	67 ± 13	38 ± 2*	18 ± 1*†	20 ± 2*†
From PEP	17 ± 4	35 ± 2*	27 ± 1*†	18 ± 2*†‡
From others	2 ± 1	2 ± 0	1 ± 1	3 ± 1
Flux toward G-6-P pool				
Total	117 ± 18	83 ± 7*	83 ± 6*	78 ± 6*
From plasma glucose	91 ± 12	42 ± 5*	31 ± 3*	38 ± 3*
From PEP	23 ± 5	39 ± 6*	48 ± 3*	34 ± 3*†‡
From others	3 ± 1	2 ± 5	2 ± 1	6 ± 4
Maximal estimation				
Glucose cycling rates	229 ± 51	56 ± 6*	37 ± 4*†	44 ± 13*†
GK flux	253 ± 32	60 ± 5*	50 ± 4*†	62 ± 6*†
G-6-Pase flux				
Total	221 ± 43	102 ± 6*	63 ± 3*†	56 ± 7*†
From plasma glucose	172 ± 32	51 ± 3*	25 ± 2*†	27 ± 3*†
From PEP	44 ± 8	48 ± 3	37 ± 2†	25 ± 3*†‡
From others	5 ± 2	3 ± 4	2 ± 1	4 ± 3
Flux toward G-6-P pool				
Total	252 ± 41	110 ± 11*	98 ± 8*	93 ± 11*
From plasma glucose	196 ± 22	55 ± 4*	38 ± 4*	45 ± 5*
From PEP	50 ± 11	52 ± 7	58 ± 6	41 ± 4
From others	6 ± 2	3 ± 0	2 ± 1	7 ± 3

The minimal estimations of the intermediate fluxes were calculated with assumption that exchange of ³H at the second position of G-6-P with hydrogen of bulk water is 100%. The maximal estimations were calculated with percent exchange of ³H at the second position of G-6-P with hydrogen of bulk water measured as the ratio of [2-³H]glucose to [3-³H]glucose incorporated into glycogen. "Others" includes possible metabolites (e.g., glycogen and glycerol) except glucose and PEP. The values for flux rates are described in $\mu\text{mol} \cdot \text{kg}^{-1} \cdot \text{min}^{-1}$ and average \pm SE of five experiments. GIR, glucose infusion rate. *Significant difference from the corresponding values of the ZCL group ($P < 0.05$). †Significant difference from the corresponding values of the ZDF-V group ($P < 0.05$). ‡Significant difference from the corresponding values of ZDF-GPI group ($P < 0.05$).

in ZDF-GPI+G). As shown in Table 1, when the efficiency of the exchange is taken into account, then in ZCL, the predicted maximal rates would be 2.4 times greater for glucose cycling and as a result, ~2.1–2.8 times greater for GK flux, total G-6-P flux, and fractional contribution to G-6-P pool from plasma glucose and PEP. In ZDF-V, ZDF-GPI, and ZDF-GPI+G, the maximal predicted rates for glucose cycling would be ~2 times greater. Given that the absolute rates of glucose cycling were much lower in these groups compared with that of ZCL, the intermediate fluxes would be predicted to be ~30–80% greater compared with the rates calculated without considering exchange efficiency. Although

this suggests the importance of measuring exchange efficiency of hydrogen at C2 position of G-6-P with that of bulk water in estimating hepatic intermediate fluxes, the problem is that the efficiency of exchange is assessed only as a ratio of [2-³H]glucose to [3-³H]glucose incorporation into glycogen, which represents an average ratio during the entire experimental period and not the desired specific point in time.

Skeletal muscle glycogen at end of the test period. The amount of incorporated plasma glucose by the direct pathway was markedly lower in ZDF-V ($0.8 \pm 0.2 \mu\text{mol}$ glucose/g muscle) compared with that in ZCL ($10.9 \pm 3.3 \mu\text{mol}$ glucose/g muscle). GPI treatment with ($1.2 \pm 0.6 \mu\text{mol}$

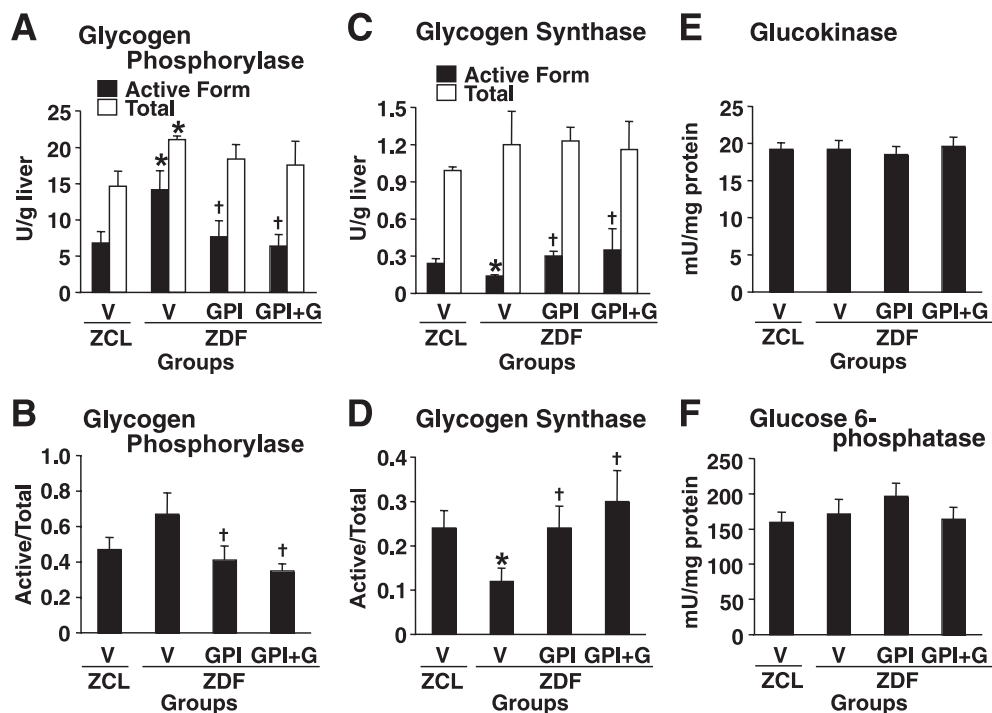


FIG. 4. Hepatic GS and phosphorylase activities in the liver at the end of the test period. Data are means \pm SE for five experiments. *Significantly different from ZCL group ($P < 0.05$). †Significantly different from ZDF-V group ($P < 0.05$).

glucose/g muscle in ZDF-GPI+G) or without (0.8 ± 0.3 μ mol glucose/g muscle in ZDF-GPI) glucose infusion did not increase the incorporation of plasma glucose into muscle glycogen.

DISCUSSION

The current study performed in an animal model of obesity-associated type 2 diabetes, ZDF, demonstrates that a failure to redirect G-6-P flux from glucose to glycogen because of reduced glycogenic flux is partially responsible for insufficient suppression of net hepatic glucose production in response to a rise in plasma glucose and insulin, but it does not explain the reduction in glucose phosphorylation.

Failure to inactivate GP α reduces both activation of GS and net glycogenesis in the presence of hyperglycemia and hyperinsulinemia in ZDF. In the presence of hyperglycemic-hyperinsulinemia associated with ZDF, markedly lower net hepatic glycogenic flux was accompanied by higher GP α activity and lower GS activity, when compared with that of ZCL clamped under similar conditions. Treatment with GPI resulted in normalized activities of these enzymes, which restored net glycogenic flux that was accompanied by marked decreases in G-6-P and UDPG content without altering total influx of metabolites toward the G-6-P pool, indicating that the normalized activity of these enzymes provides a “pull mechanism” for glycogen synthesis. Therefore, a defect in net glycogenesis in response to hyperglycemic-hyperinsulinemia observed with ZDF might arise from a failure to regulate GS and/or GP activity and not from a lower influx of metabolites toward the G-6-P pool.

The treatment with the GPI (CP-368298), which binds to the indole inhibitor site of GP (20), caused not only decreased activity of GP α but also increased activity of GS

in liver in ZDF. This is thought to occur as a result of the binding-induced conformational changes that make GP α better substrate for its regulatory phosphatase, protein phosphatase 1 (PP1) (21), and/or interfere with the binding of GP α to a potent allosteric inhibitory site of PP1, the COOH-terminal domain of the glycogen-targeting subunit of PP1 (22–26). Because activation of GS is mediated by dephosphorylation of the enzyme by PP1, the activation of GS by GPI may result from decreased GP α inhibition of PP1. Therefore, a defect in net glycogenic flux in response to hyperglycemia and hyperinsulinemia in ZDF may arise from a failure of glucose and/or insulin to inactivate GP α .

Insulin inactivates GP α by activating PP1 via the activation of PKB/Akt (27). It was reported that insulin stimulated activation of PKB/Akt is blunted in the liver of ZDF (28). Thus, the impaired insulin signaling may be responsible for the failure of the hormone to activate GS. On the other hand, glucose inhibits GP α by binding to the catalytic site of the enzyme (29) and stabilizing the enzyme by changing the active form to an inactive form that is a better substrate for PP1 (30). Hepatocyte intracellular glucose concentration is always similar or slightly higher compared with plasma concentration of the sugar (31,32), which predicts that ZDF would have very high hepatic intracellular glucose concentrations because their plasma glucose levels were ~ 19 mmol/L. It still remains unknown how GP α remains in its phosphorylated active form given the presence of both hyperinsulinemia and hyperglycemia in ZDF.

A lack of net glycogenic flux contributes to insufficient suppression of net hepatic glucose production by failing to redirect G-6-P flow from glucose to glycogen in ZDF. Restoration of net glycogenic flux decreased EGP in ZDF treated with GPI. Net hepatic glucose flux is the balance between glucose phosphorylation catalyzed by GK and G-6-P

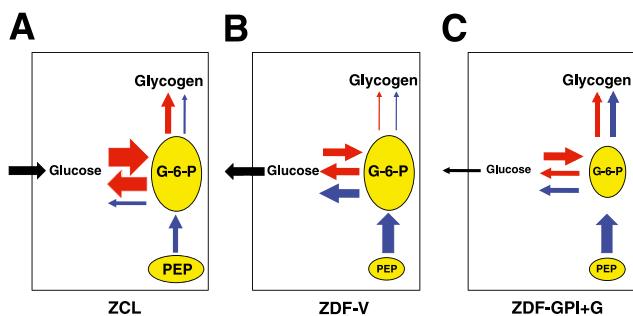


FIG. 5. Altered intermediate fluxes by inhibiting GPa in liver of ZDF in the presence of hyperglycemia and hyperinsulinemia. Described fluxes are the minimal estimations. Black arrows, net hepatic glucose flux; red arrows, flux of taken up glucose; and blue arrows, PEP flux. **A:** ZCL. When plasma glucose and insulin levels were raised to that in ZDF, total flux toward G-6-P pool consists of two major fractions, plasma glucose (78%) and PEP (20%). Of the G-6-P derived from plasma glucose, 26% of G-6-P is stored as glycogen and the rest (74%) recycle back to glucose. Of the G-6-P derived from PEP, 26% is stored as glycogen and the rest (74%) is released as glucose. GK flux (glucose to G-6-P) was higher than G-6-Pase flux, leading to net hepatic glucose uptake. **B:** ZDF-V. Compared with ZCL, total flux toward the G-6-P pool, consisting of lower fractions of plasma glucose (50%) and higher fractions of PEP (47%), was significantly lower. Total efflux from G-6-P pool flowed primarily toward glucose (90%) and glycogen (10%). Of the G-6-P derived from plasma glucose, only 10% was stored as glycogen and the rest (90%) was recycled to glucose. Of the G-6-P derived from PEP, 10% was stored as glycogen and the rest (90%) was released as glucose. The flux from plasma glucose to G-6-P was ~30%, and the flux from PEP to G-6-P was double of that in ZCL, whereas G-6-Pase flux was similar. GK flux was lower than G-6-Pase flux contrary to ZCL, leading to net hepatic glucose production. **C:** ZDF-GPI+G. Compared with ZDF-V, total flux toward the G-6-P pool was similar with similar fraction of plasma glucose and PEP. On the other hand, the efflux from G-6-P pool flowed toward glycogen was five times higher and in contrast, the efflux from G-6-P toward plasma glucose was about half. GK flux balanced with G-6-Pase flux, leading to decreased net hepatic glucose production.

dephosphorylation catalyzed by G-6-Pase. The reduction of hepatic glucose production by restored net glycogenesis was associated with decreased G-6-Pase flux and content of its substrate, G-6-P. The decreased G-6-P content was accompanied by no alteration of the total flux through the G-6-P pool. During steady state, the efflux rate equals the influx rate as a result of equilibration between the substrate (G-6-P) concentration and the catalytic activity (V_{max} and K_m) of the rate-regulating enzymes of glycogen synthesis, glycolysis, and pentose phosphate pathway along with G-6-Pase. The activation of GS may shift the equilibrium in favor of increased glycogenic flux and lower G-6-P concentration. As a result of this reduced G-6-P concentration, the fluxes of the other pathways are decreased and a new steady state is established without altering total flux through the G-6-P pool. Therefore, increased efflux of G-6-P to glycogen by a pull mechanism likely decreased cytoplasmic G-6-P concentration, resulting in decreased G-6-Pase flux.

Reduced glucose phosphorylation and elevated total gluconeogenesis are not secondary to a defect in net glycogenic flux in ZDF. Flux from plasma glucose toward the G-6-P pool and the percent contribution of plasma glucose to form UDPG in liver of ZDF were one-third and two-thirds of that in ZCL, respectively. Total gluconeogenesis (PEP to G-6-P) in ZDF was 50% higher than that of ZCL. The restoration of glycogenic flux does not alter these parameters at all in ZDF. The redirection of G-6-P flux by restoring net glycogenic flux did not alter the relative contribution of PEP and plasma glucose (glucose recycling) to plasma glucose (90 and 90% in ZDF-V

compared with 53 and 52% in ZDF-GPI+G, respectively) and to glycogen (10 and 10% in ZDF-V compared with 47 and 48% in ZDF-PG-G, respectively). Therefore, the blunted response of glucose phosphorylation to hyperglycemia and the increased total gluconeogenesis seen in ZDF is not likely a result of defective glycogenic flux.

A failure to increase glucose phosphorylation explains insufficient suppression of net hepatic glucose production in ZDF. As seen in patients with type 2 diabetes (5,6), ZDF, compared with ZCL, exhibit a lower increment in net flux from glucose to glycogen in response to hyperglycemia and hyperinsulinemia that is associated with a decrease in both GK flux and UDPG flux (10–14). The lowered net flux is restored by normalizing GK activity (10–13) or by activating GS (14). The current study shows that reduced glucose phosphorylation by GK is not the result of reduced glycogenic flux. These results suggest that impaired activation of both glycogenesis and glucose phosphorylation are involved.

ACKNOWLEDGMENTS

M.S. has received a grant from the National Institutes of Health (NIH; DK-60667). The hormone assay core laboratory at Vanderbilt University Medical Center is supported by a grant from the NIH (DK-20593). K.L.H. and J.L.T. were employees of Pfizer. Pfizer supplied GPI (CP-368296) for this study and approved the current study presented. K.L.H. and J.L.T. contributed toward development of this GPI, and J.L.T. discussed how to administer this GPI to animals. No other potential conflicts of interest relevant to this article were reported.

T.P.T., Y.F., and E.P.D. researched data. R.L.P. reviewed and edited the manuscript. K.L.H. researched data. J.L.T. researched data and contributed to discussion. M.S. researched data and wrote the manuscript.

REFERENCES

1. Consoli A. Role of liver in pathophysiology of NIDDM. *Diabetes Care* 1992; 15:430–441
2. Ferrannini E, Groop LC. Hepatic glucose production in insulin-resistant states. *Diabetes Metab Rev* 1989;5:711–726
3. Iozzo P, Hallsten K, Oikonen V, et al. Insulin-mediated hepatic glucose uptake is impaired in type 2 diabetes: evidence for a relationship with glycemic control. *J Clin Endocrinol Metab* 2003;88:2055–2060
4. Firth RG, Bell PM, Marsh HM, Hansen I, Rizza RA. Postprandial hyperglycemia in patients with noninsulin-dependent diabetes mellitus. Role of hepatic and extrahepatic tissues. *J Clin Invest* 1986;77:1525–1532
5. Basu A, Basu R, Shah P, et al. Type 2 diabetes impairs splanchnic uptake of glucose but does not alter intestinal glucose absorption during enteral glucose feeding: additional evidence for a defect in hepatic glucokinase activity. *Diabetes* 2001;50:1351–1362
6. Basu A, Basu R, Shah P, et al. Effects of type 2 diabetes on the ability of insulin and glucose to regulate splanchnic and muscle glucose metabolism: evidence for a defect in hepatic glucokinase activity. *Diabetes* 2000;49: 272–283
7. Krssak M, Brehm A, Bernroider E, et al. Alterations in postprandial hepatic glycogen metabolism in type 2 diabetes. *Diabetes* 2004;53:3048–3056
8. Agius L. Glucokinase and molecular aspects of liver glycogen metabolism. *Biochem J* 2008;414:1–18
9. Mevorach M, Giacca A, Aharon Y, Hawkins M, Shamoon H, Rossetti L. Regulation of endogenous glucose production by glucose per se is impaired in type 2 diabetes mellitus. *J Clin Invest* 1998;102:744–753
10. Fujimoto Y, Donahue EP, Shiota M. Defect in glucokinase translocation in Zucker diabetic fatty rats. *Am J Physiol Endocrinol Metab* 2004;287:E414–E423
11. Fujimoto Y, Torres TP, Donahue EP, Shiota M. Glucose toxicity is responsible for the development of impaired regulation of endogenous glucose production and hepatic glucokinase in Zucker diabetic fatty rats. *Diabetes* 2006;55:2479–2490

12. Shin JS, Torres TP, Catlin RL, Donahue EP, Shiota M. A defect in glucose-induced dissociation of glucokinase from the regulatory protein in Zucker diabetic fatty rats in the early stage of diabetes. *Am J Physiol Regul Integr Comp Physiol* 2007;292:R1381–R1390
13. Torres TP, Catlin RL, Chan R, et al. Restoration of hepatic glucokinase expression corrects hepatic glucose flux and normalizes plasma glucose in Zucker diabetic fatty rats. *Diabetes* 2009;58:78–86
14. Cline GW, Johnson K, Regittinig W, et al. Effects of a novel glycogen synthase kinase-3 inhibitor on insulin-stimulated glucose metabolism in Zucker diabetic fatty (fa/fa) rats. *Diabetes* 2002;51:2903–2910
15. Hother-Nielsen O, Henriksen JE, Holst JJ, Beck-Nielsen H. Effects of insulin on glucose turnover rates in vivo: isotope dilution versus constant specific activity technique. *Metabolism* 1996;45:82–91
16. Katz J, Dunn A, Chenoweth M, Golden S. Determination of synthesis, recycling and body mass of glucose in rats and rabbits in vivo 3H- and 14C-labelled glucose. *Biochem J* 1974;142:171–183
17. Steele R, Bishop JS, Dunn A, Altszuler N, Rathbeb I, Debodo RC. Inhibition by insulin of hepatic glucose production in the normal dog. *Am J Physiol* 1965;208:301–306
18. Katz J, Wood HG. The use of glucose-C14 for the evaluation of the pathways of glucose metabolism. *J Biol Chem* 1960;235:2165–2177
19. Katz J, Wood HG. The use of C14O2 yields from glucose-1- and -6-C14 for the evaluation of the pathways of glucose metabolism. *J Biol Chem* 1963;238:517–523
20. Treadway JL, Mendys P, Hoover DJ. Glycogen phosphorylase inhibitors for treatment of type 2 diabetes mellitus. *Expert Opin Investig Drugs* 2001;10:439–454
21. Kasvinsky PJ, Fletterick RJ, Madsen NB. Regulation of the dephosphorylation of glycogen phosphorylase a and synthase b by glucose and caffeine in isolated hepatocytes. *Can J Biochem* 1981;59:387–395
22. Brady MJ, Saltiel AR. The role of protein phosphatase-1 in insulin action. *Recent Prog Horm Res* 2001;56:157–173
23. Pautsch A, Stadler N, Wissdorf O, Langkopf E, Moreth W, Streicher R. Molecular recognition of the protein phosphatase 1 glycogen targeting subunit by glycogen phosphorylase. *J Biol Chem* 2008;283:8913–8918
24. Kelsall IR, Munro S, Hallyburton I, Treadway JL, Cohen PT. The hepatic PP1 glycogen-targeting subunit interaction with phosphorylase a can be blocked by C-terminal tyrosine deletion or an indole drug. *FEBS Lett* 2007;581:4749–4753
25. Zibrova D, Grempler R, Streicher R, Kauschke SG. Inhibition of the interaction between protein phosphatase 1 glycogen-targeting subunit and glycogen phosphorylase increases glycogen synthesis in primary rat hepatocytes. *Biochem J* 2008;412:359–366
26. Armstrong CG, Doherty MJ, Cohen PT. Identification of the separate domains in the hepatic glycogen-targeting subunit of protein phosphatase 1 that interact with phosphorylase a, glycogen and protein phosphatase 1. *Biochem J* 1998;336:699–704
27. Aiston S, Hampson LJ, Arden C, Iynedjian PB, Agius L. The role of protein kinase B/Akt in insulin-induced inactivation of phosphorylase in rat hepatocytes. *Diabetologia* 2006;49:174–182
28. Nawano M, Oku A, Ueta K, et al. Hyperglycemia contributes insulin resistance in hepatic and adipose tissue but not skeletal muscle of ZDF rats. *Am J Physiol Endocrinol Metab* 2000;278:E535–E543
29. Ercan-Fang N, Gannon MC, Rath VL, Treadway JL, Taylor MR, Nuttall FQ. Integrated effects of multiple modulators on human liver glycogen phosphorylase a. *Am J Physiol Endocrinol Metab* 2002;283:E29–E37
30. McCormack JG, Westergaard N, Kristiansen M, Brand CL, Lau J. Pharmacological approaches to inhibit endogenous glucose production as a means of anti-diabetic therapy. *Curr Pharm Des* 2001;7:1451–1474
31. Wals PA, Katz J. A concentration gradient of glucose from liver to plasma. *Metabolism* 1993;42:1492–1496
32. Niewoehner CB, Nuttall FQ. Relationship of hepatic glucose uptake to intrahepatic glucose concentration in fasted rats after glucose load. *Diabetes* 1988;37:1559–1566